A New Manufacturing Technology for Induction Machine Copper Rotors

John S. Hsu, E. A. Franco-Ferreira, Chester L. Coomer, and S. Michael Jenkins Sr.

Oak Ridge National Laboratory
2360 Cherahala Boulevard
Knoxville, Tennessee 37932

Key words: *Induction motors, Copper rotor, Aluminum rotor, Friction weld, High efficiency, Energy savings.*

Abstract

The benefits of energy and operational cost savings from using copper rotors are well recognized. The main barrier to die casting copper rotors is short mold life. This paper introduces a new approach for manufacturing copper-bar rotors. Either copper, aluminum, or their alloys can be used for the end rings. Both solid-core and laminated-core rotors were built. High quality joints of aluminum to copper were produced and evaluated. This technology can also be used for manufacturing aluminum bar rotors with aluminum end rings. Further development is needed to study the life time reliability of the joint, to optimize manufacturing fixtures, and to conduct large-rotor tests.

I. INTRODUCTION

Carbon dioxide (CO_2) is thought to be a key greenhouse gas responsible for global warming. Most man-made CO_2 emissions comes from burning fossil fuels, such as oil, coal and gas. When we save on energy use, we help to reduce CO_2 emissions and other forms of air pollution. Energy efficiency also saves consumers and businesses millions of dollars in energy costs each year.

Motor-driven systems consume about two-thirds of the electricity generated in the United States. The expected popularity of electric vehicles will significantly increase the use of electric motors. Energy efficiency improvements for all types of electric motors will become increasingly important.

The basic losses in an induction motor consist of resistance losses in the stator winding and rotor cage, iron losses, friction and windage losses, and stray-load loss. The resistivities of copper and aluminum per circular mil, per foot at 20°C are 10.37Ω and 16.06Ω, respectively. Hence, for the same current requirement, the substitution of copper for aluminum results in (16.06-10.37)/16.06=35.4% reduction in resistance loss.

Poloujadoff et al. [1] made economic comparisons between aluminum and copper squirrel cages. They concluded that when the initial cost is considered, the initial price of copper cages is higher by 30%, but the savings in operating losses is seven or eight times the increase in price.

Lie and Pietro [2] pointed out that significant motor efficiency improvement could be achieved by substituting copper for aluminum in a die-cast rotor for a squirrel cage induction motor. Their test, conducted on a 10-hp, 4-pole motor, shows the actual efficiency gain is 4.4 percentage points at quarter load, 2.4 percentage points at half load, 1.8 percentage points at three-quarter load, and 1.5 percentage points at full load. This translates to loss reductions of 15% at half load and 10% at full load. Their 1995 assessment on the barriers to high efficiency motors were: initial cost ranging from 30 to 90 percent higher, lack of awareness, overlooked long term financial benefit, and longer delivery time due to low demand. However, today's assessment, at least in the United States, may have been changed due to the EPAC law that requires a minimum efficiency for the most commonly used new motors (i.e., 1-200 hp, standard induction motors) sold in the United States. The law has certainly affected the users' awareness and willingness to pay for a higher efficiency motor.

On the basis of the 10% to 15% reductions of motor losses, a potential for saving 200 trillion BTU/year may be achieved. Thus, the potential benefits from using copper rotors are significant.

At the present time, NEMA-frame-size [4] motors are generally produced with die cast aluminum rotors. For larger motors, expensive brazed copper rotors are used.

Research sponsored by the Oak Ridge National Laboratory managed by UT-Battelle, LLC for the U. S. Department of Energy under contract DE-AC05-00OR22725.

The main barrier to die casting copper rotors is short mold life, because the melting point of copper is 1083°C, much higher than the 660°C melting point of aluminum.

II. FRICTION WELDING OF A DISCONTINUOUS SURFACE

Friction welding is a well-established process for rapidly joining two metal surfaces which possess rotational symmetry. The surfaces to be joined are normally continuous. The materials to be joined can be either similar or dissimilar. The joint produced by the process has the nature of a forge-weld in that no melting of either of the joint components occurs.

Friction welding is accomplished by forcing one of the joint components, which is rotating, against the other joint component, which is stationary. The frictional heat thus generated softens the joint surfaces and enables the production of a solid state bond under the action of the forging force.

A complication is introduced into the normal friction welding process when it is applied to the fabrication of electric motor rotors. The end ring, which must be welded to the conductor bars, has a continuous surface; the ends of the conductor bars constitute a discontinuous surface. This type of joint configuration is not normally encountered in friction welding applications and extensive development work was required to perfect the techniques for obtaining sound joints. The work resulted in the issuance of a U. S. Patent [3] dealing specifically with the fabrication of squirrel cage rotors by friction welding solid end rings to the ends of conductor bars filling the core slots. The process is applicable to any combination of copper, aluminum or their alloys.

Fig. 1 illustrates the friction weld setup for making a squirrel-cage rotor. In this instance the rotor has copper conductor bars and aluminum end rings. The rotor core, composed of a lamination stack with its slots filled by copper bars, is held in a stationary collet. A back stop prevents axial movement of the copper bars. The aluminum end ring is held in a rotating collet, also equipped with a back stop, which is brought to a preset speed and then allowed to free-wheel. As soon as the drive is de-clutched the end ring is forced against the rotor end with a preset amount of force. The rotation of the end ring is brought to a stop by the ensuing friction between the two joint components, and if the system parameters have been chosen correctly, a sound joint results between the end ring and the ends of all the copper bars.

A significant challenge during the development of the process was caused by the fact that the ends of the conductor bars had to protrude a short distance from the ends of the rotor core. Too much protrusion resulted in excessive deformation of the bar ends which reduced the areas of the joints to less than the areas of the bars. Too little protrusion resulted in no joint at all.

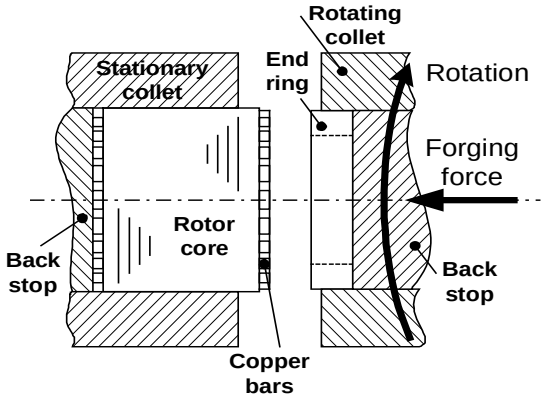

Fig. 1 Friction weld setup for making squirrel-cage rotor

III. COPPER BARS WITH ALUMINUM END RINGS

Using the process described above, motor rotors may certainly be produced with copper conductor bars and copper end rings. However, there may be an opportunity for cost reduction in using aluminum end rings with copper conductor bars. An aluminum end ring would require at least a 55% larger cross sectional area than a copper one due to its lower conductivity. However, because the density of copper is 3.29 times that of aluminum the weight of the larger aluminum end ring would be only 47% that of a copper ring. Based on recent pricing of copper and aluminum (copper @ $0.86/lb vs aluminum @ $0.73/lb), an aluminum end ring is estimated to cost 60% less than its copper equivalent. As shown in Fig. 2 conventional induction motors have ample space for the larger end rings required with the use of aluminum.

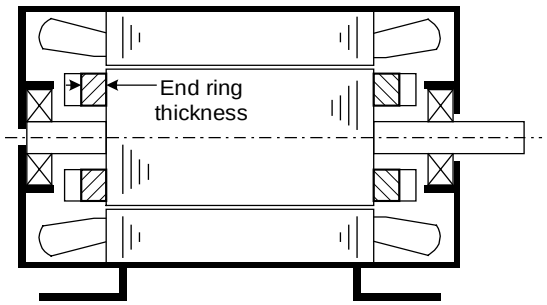

Fig. 2 Available space for thicker end ring.

In the case of large brazed copper rotors, pure copper bars are commonly used with copper alloy end rings, whose higher resistivity provides a higher starting torque and lower starting current. Thermal stresses during starting do not result in any cracking in the brazed joints. The quality and strength of a friction-welded joint can be expected to be equal to or surpass that of a brazed joint. However, when there is a difference in coefficient of thermal expansion

(CTE), as in the case of copper bars and aluminum rings, further investigation of the thermal stress situation will be required.

IV. PROTOTYPE ROTORS

Two types of rotor cores were used for prototypes during the development of the fabrication techniques. Initial work was carried out on solid-core rotor mock-ups. This work would be applicable to the inverse rotors used in direct-drive electric-vehicle induction motors. The results obtained in the solid-core work were then used as a basis for development of techniques for producing laminated-core rotors used in conventional induction motors.

4.1 Solid-Core Rotors

A series of solid-core rotor mock-ups was welded to develop the techniques and parameters for making sound joints between the ends of an array of copper conductor bars and a continuous aluminum end ring. Each mock-up consisted of a 1.5" long x 1.25" diameter cylinder of plain carbon steel. The six conductor bars were 0.25" diameter copper rods located on a 7/8" diameter circle. Each core had a 0.5" diameter hole running longitudinally through its center. The end rings were 1.25" diameter cylinders of 6061-T6 aluminum with a 0.5" diameter bore. The physical set-up used for the friction welding of these mock-ups was identical to that shown in Fig. 1. A longitudinal cross section of a typical solid-core rotor mock-up is shown in Fig. 3.

During the course of the investigation a number of variables, namely, the conductor bar stick-out, flywheel moment of inertia, rotational speed and weld load (forging force), were studied. Joint quality was evaluated by making metallographic examinations of each bar-to-end ring joint in the mock-ups.

Once satisfactory results were obtained for the 1.25" diameter mock-ups, larger mock-ups, i.e., 1.466" long x 1.790" diameter, were made to establish parameters for making actual laminated-core motor rotors. These solid-core mock-ups each had nine 3/8" diameter copper conductor bars located on a 1.25" diameter circle. The end rings were made from 1.790" diameter 6061-T6 aluminum cylinders with ¾" diameter bores.

Because the size of these mock-ups exceeded the capacity of the available friction welder at ORNL, all subsequent welding operations were carried out at the facility of the manufacturer of the friction welding equipment.

Once again, bar projection distance, moment of inertia, speed and load were investigated. The parameters which produced the best joints, based on metallographic examination at ORNL, were used as the basis for the welding of actual laminated-core rotors with the same dimensional envelope as the solid-core mock-ups. The optimized parameters from this series of tests were: bar stick-out of 0.030, moment of inertia of 101.9 lb-ft^2, speed of 1,550 rpm, and load of 51,920 lbs.

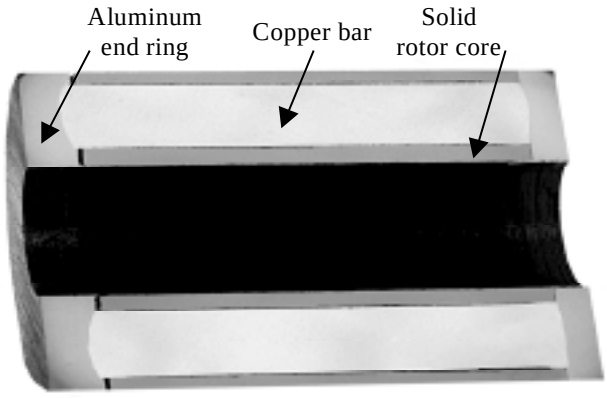

Fig. 3 Longitudinal cross section of rotor with solid core, copper bars, and aluminum end rings.

4.2 Laminated-Core Rotors

The cores for the rotors used in this portion of the program were obtained by chemically etching the aluminum end rings and conductor bars out of laminated cores from actual induction motors. Once the cores had been prepared, custom-made copper conductor bars were hand-inserted into the slots in the cores. Fig. 4 is a side view of a rotor after bar insertion, but prior to trimming of the ends of the the bars to the correct stick-out. Fig. 5 is an end view of the same rotor. The bars were contoured by hand to approximate the shape of the rotor slots. The absence of a tight fit-up, giving an estimated 85% fill-factor, is apparent in Fig. 5.

The rotor assembly was sent to the welding vendor in the condition shown in Figs. 4 and 5. The vendor faced off the ends of the conductor bars to the required 0.015/0.030 inch stick-out just prior to welding. The welding parameters which were used on this rotor were: moment of inertia of 101.9 lb-ft^2, speed of 1,685 rpm, and load of 28,910 lbs. After welding the rotor was returned to ORNL for machining of the end rings. These end rings were made thick enough to compensate for the resistivity difference (1.86 times) between 6061-T6 aluminum alloy and copper. The final-machined rotor, prior to installation of the shaft, is shown in Fig. 6. There was some relative rotation of the laminations, especially at the ends of the rotor, under the influence of the welding torque. This effect was due to the failure of the stationary collet to grip the rotor body tightly enough. This is a problem which is not considered to be insoluble.

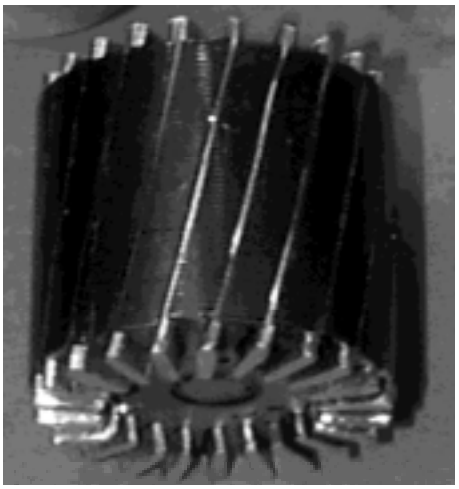

Fig. 4 Laminated rotor core with inserted copper bars.

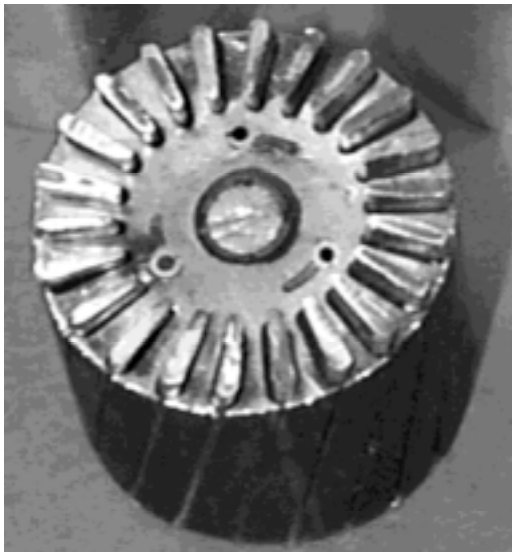

Fig. 5 Top view showing 85% fill-factor copper bars and slots.

V. TEST RESULTS

5.1 Joint Evaluation:

As stated above, joint quality throughout the program was determined by metallographic evaluation. The metallographic evaluation was found to be quite definitive in that all voids, cracks, and unwelded areas were easily detectable. In addition, the thickness of the intermetallic layer at the joint interface was measurable. In the case of copper to aluminum, an interfacial layer of the intermetallic compound, $CuAl_2$, is always formed.

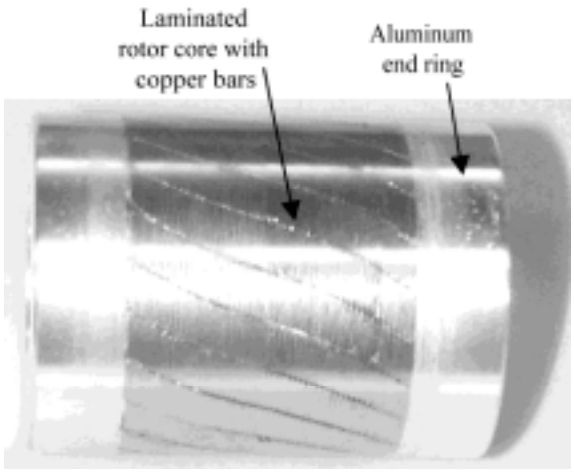

Fig. 6 Copper-bar rotor with aluminum end rings and laminated core.

The thickness of this layer depends on the time/temperature characteristics of the welding process. Since all intermetallic compounds are brittle, it is important that the thickness of the layer be minimized. This is done through suitable manipulation of the welding parameters.

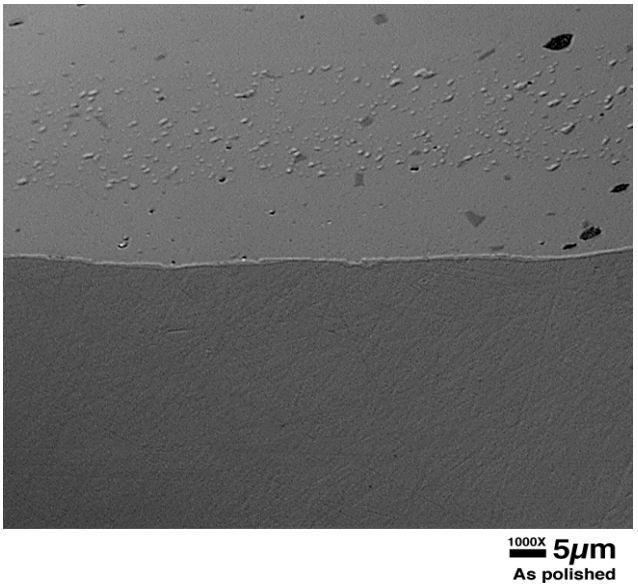

Fig. 7 Cross section of a solid-rotor-core, aluminum-copper joint.

Fig. 7 shows the appearance of a typical satisfactory aluminum-copper joint. In this case the joint is between a 0.375" diameter copper bar and the 6061-T6 aluminum end ring in one of the solid-core rotor mock-ups welded by the welding vendor. The aluminum is at the top of the figure with the 0.00002" thick intermetallic layer running across the midplane. With a layer of this thickness the bulk mechanical properties of the joint are determined by the

properties of the aluminum and the copper rather than by the properties of the $CuAl_2$.

5.2 Rotor Cage Electrical Conductivity:

A single phase of the stator windings was used throughout all tests to provide a directional flux for a uniform test capability.

The laminated-core prototype is a 2-pole rotor composed of 22 approximately 85% fill-factor copper bars with 6061-T6 aluminum end rings. The tests are designed to compare the rotor-cage conductivity of the prototype with that of a die-cast aluminum-cage rotor made of identical punchings. Both rotors were inserted into the same stator bore successively for their locked-rotor tests.

The rotor used for the open-rotor-cage test was the same die-cast aluminum-cage rotor with its end rings machined off. The rotor was inserted into the stator bore for the test. Because the rotor was stationary during this test, the rotor core loss is included to have a situation similar to that for the locked-rotor tests.

5.2.1 Rotor Resistance Evaluation Method:

This section presents the derivation of the evaluation method for obtaining the tested rotor-resistance value. The equivalent circuit of an induction motor is like a transformer with the stator being the primary and the rotor the secondary. The rotor resistance can be evaluated by conducting locked-rotor tests and open-rotor-cage tests. The test data are given in the Appendix. The following derivation gives a method for the rotor resistance evaluation.

Fig. 8a shows the locked-rotor equivalent circuit. The circuit can be redrawn as shown in Fig. 8b, where the resistance of both the rotor and core circuits, R_{2+core}, yields

$$R_{2+core} := \text{Real}\left[\frac{\left(j\cdot X_2 + R_2\right)\cdot\left(j\cdot X_m + R_m\right)}{j\cdot\left(X_2 + X_m\right) + R_2 + R_m}\right] \qquad (1)$$

Where the symbol ":=" printed from a computer software means "=" for equations. That software uses "=" to find the numerical answers.

The reactance of both the rotor and core circuits, X_{2+core}, is the imaginary part. It equals

$$X_{2+core} := \text{Imag}\left[\frac{\left(j\cdot X_2 + R_2\right)\cdot\left(j\cdot X_m + R_m\right)}{j\cdot\left(X_2 + X_m\right) + R_2 + R_m}\right] \qquad (2)$$

The stator resistance, R_1, can be measured with an ohmmeter. The locked-rotor impedance, Z_{locked}, is the ratio of the locked-rotor voltage and current.

$$Z_{locked} := \frac{V_{locked}}{I_{locked}} \qquad (3)$$

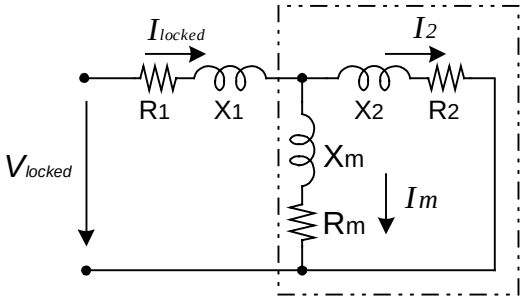

(a) Locked-rotor

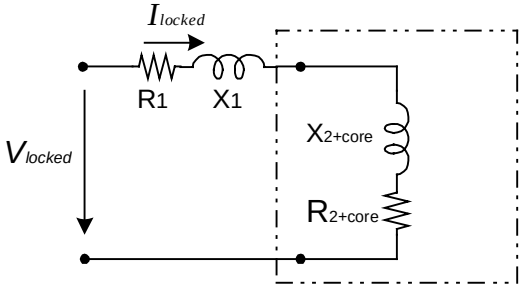

(b) Redrawn locked-rotor

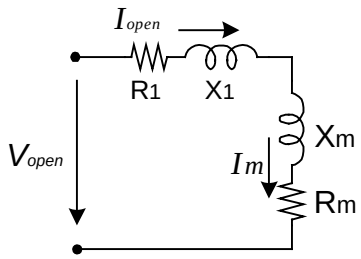

(c) Open-rotor-cage circuit

Fig. 8 Equivalent circuits: (a) locked-rotor, (b) redrawn locked-rotor, and (c) open-rotor-cage.

The locked-rotor resistance, R_{locked}, is obtained from the locked-rotor power and current.

$$R_{locked} := \frac{P_{locked}}{\left(I_{locked}\right)^2} \qquad (4)$$

The locked-rotor reactance yields

$$X_{locked} := \sqrt{\left(Z_{locked}\right)^2 - \left(R_{locked}\right)^2} \qquad (5)$$

Assuming that the stator leakage reactance, X_1, and the rotor leakage reactance, X_2, are equal and their summation equals X_{locked}, we have

$$X_1 := \frac{X_{locked}}{2} \qquad (6)$$

and

$$X_2 := \frac{X_{locked}}{2} \quad (7)$$

Referring to Fig. 8b the resistance, R_{2+core}, is

$$R_{2+core} := R_{locked} - R_1 \quad (8)$$

From the open-rotor-cage test, the impedance, Z_{open}, as shown in Fig. 8c is the ratio of the corresponding voltage and current.

$$Z_{open} := \frac{V_{open}}{I_{open}} \quad (9)$$

Z_{open} contains a resistance component, R_{open}, and a reactance component, X_{open}. They are

$$R_{open} := \frac{P_{open}}{(I_{open})^2} \quad (10)$$

and

$$X_{open} := \sqrt{(Z_{open})^2 - (R_{open})^2} \quad (11)$$

Referring to Fig. 8c the following two equations can be obtained.

$$R_m := R_{open} - R_1 \quad (12)$$

$$X_m := X_{open} - X_1 \quad (13)$$

The above equations are sufficient to calculate all the parameters on both sides of eqn. (1) except the rotor resistance, R_2. R_2 can thus be solved from eqn. (1) through iteration.

$$R_{2+core} := Real\left[\frac{(j \cdot X_2 + R_2) \cdot (j \cdot X_m + R_m)}{j \cdot (X_2 + X_m) + R_2 + R_m}\right] \quad (1)$$

5.2.2 Tested Rotor-Resistance Values:

Fig. 9 shows the tested rotor-resistance comparison between the copper-bars/aluminum-rings rotor and the cast-aluminum rotor. The copper-bars/aluminum-rings rotor has lower resistance. The resistance ratios corresponding to the low-resistance rotor over the cast-aluminum rotor are given in the Table 1.

The average rotor resistance ratio from Table 1 is 0.72 which is close to the expected 0.58/0.85=0.68 ratio derived from the estimated 85%-filled copper bars and the 58% of aluminum's resistivity. The ratio of 0.72/0.68=1.06 shows a 6% discrepancy. However, in view of the inaccuracy of the fill-factor estimate and uncertainties as to the actual conductivities of the alloys used to fabricate the rotor, this discrepancy is considered to be insignificant.

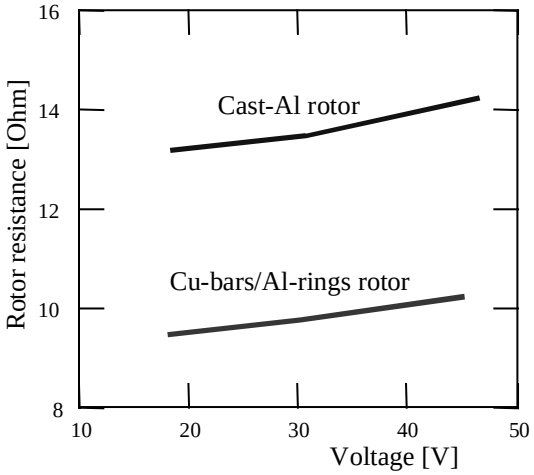

Fig. 9 Tested rotor resistances

V_{locked}	18.1 V	30.1 V	45.2 V
R_2 ratio	0.718	0.724	0.718

Table 1 Rotor resistance ratios at different test voltages.

5.2.3 Rotor Cage Uniformity Tests:

In order to determine the quality of the joints around the rotor, the stator voltage, current, and wattage at 0, 45, and 90-degree positions of the rotor with respect to an arbitrary stator axis were taken at different voltages. The variations of current, I_{locked}, and power, P_{locked}, at different angular positions shown in the Appendix are small and do not indicate any significant difference between the die-cast rotor and the copper-bars/aluminum-rings rotor.

IV. CONCLUSIONS.

- The benefits of energy and operational cost savings from using copper rotors are well recognized.
- The main barrier to die casting copper rotors is short mold life, because the melting point of copper is 1083°C, much higher than the 660°C melting point of aluminum.
- This paper introduces a new approach for manufacturing copper-bar rotors.
- Either copper, aluminum, or their alloys can be used for the end rings.
- Both solid-core and laminated-core rotors were built.
- High quality joints of aluminum to copper were produced and preliminarily evaluated.
- This technology can also be used for manufacturing aluminum bar rotors with aluminum end rings.
- Further development is needed to study the life time reliability of the joint, to optimize manufacturing fixtures, and to conduct large rotor tests.

V ACKNOWLEDGMENT

The authors appreciate the support funded by the Office of Advanced Automotive Technologies, Department of Energy. We are obliged for the donation and permission for purchasing punchings from the Baldor Electric Company and the General Electric Company. Thanks are given to Manufacturing Technology, Inc for assistance in prototype production and to Mr. M. T. Gresham for assistance in friction welding development. Encouragement from the Power Electronics and Electric Machines Research Center headed by Mr. Donald Adams is gratefully acknowledged.

VI. REFERENCE

[1] M. Poloujadoff, J. C. Mipo, M. Nurdin, "Some Economical Comparisons between Aluminum and Copper Squirrel Cages," IEEE Transactions on Energy Conversion, Vol. 10, No. 3, September 1995, pp. 415-418.

[2] Sian Lie, Carlo Di Pietro, "Copper Die-Cast Rotor Efficiency Improvement and Economic Consideration," IEEE Transactions on Energy Conversion, Vol. 10, No. 3, September 1995, pp. 419-424.

[3] John S. Hsu, Edgard A. Franco-Ferreira, "Method of Manufacturing Squirrel Cage Rotors," U.S. Patent No. 6,088,906, July 18, 2000.

[4] NEMA Standards Publication No. MG1, National Electrical Manufacturers Association (NEMA), Washington, D.C., 1993.

VIII. APPENDIX

8.1 Locked-Rotor Test Data:

Copper-bars/Aluminum-rings rotor			
Remarks	V_{locked} [V]	I_{locked} [A]	P_{locked} [W]
0°	18.06	0.6148	8.0
45°	18.12	0.6223	8.1
90°	18.12	0.6212	8.1
Average	18.10	0.6194	8.1
X_{Locked}=20.3 Ω		R_{2+core}=8.3 Ω	
0°	30.11	1.0478	23.4
45°	30.03	1.0369	22.9
90°	30.11	1.0475	23.2
Average	30.08	1.0441	23.2
X_{Locked}=19.5 Ω		R_{2+core}=8.6 Ω	
0°	45.15	1.6159	55.6
45°	45.29	1.5706	53.6
90°	45.28	1.5467	52.6
Average	45.24	1.5777	53.9
X_{Locked}=18.8 Ω		R_{2+core}=9.0 Ω	
Cast Aluminum rotor			
Remarks	V_{locked} [V]	I_{locked} [A]	P_{locked} [W]
0°	18.32	0.6089	8.9
90°	18.32	0.6088	8.9
Average	18.32	0.6088	8.9
X_{Locked}=18.1 Ω		R_{2+core}=11.3 Ω	
0°	30.71	1.0114	24.7
90°	30.90	1.0143	25.0
Average	30.80	1.0129	24.9
X_{Locked}=18.4 Ω		R_{2+core}=11.5 Ω	
0°	46.61	1.5104	56.5
90°	46.62	1.5060	56.4
Average	46.62	1.5082	56.5
X_{Locked}=18.4 Ω		R_{2+core}=12.1 Ω	

8.2 Open-Rotor-Cage Test Data:

V_{open} [V]	I_{open} [A]	P_{open} [W]	X_{open} [Ω]
18.37	0.1374	1.5	107.3
30.12	0.2268	4.2	104.7
30.73	0.2314	4.4	104.3
45.23	0.3461	10.0	100.5
46.63	0.3569	10.7	100.1